Heredia et al., J Material Sci Eng 2016, 5:6
DOI: 10.4172/2169-0022.1000286

Journal of Material Sciences & Engineering

Research Article Open Access

Stress-Strain Characterization in Fiber-Reinforced Composites by Digital Image Correlation

Heredia AS[1], Aguilar PAM[2*] and Ocampo AM[2]

[1]Research Center on Engineering and Applied Sciences - (IICBA)
[2]Department of Engineering, Autonomous Univiersity of Morelos State, Mexico

Abstract

Composite materials are widely used in structural mechanics as they can withstand high loads; although after a while, they can present relative strain due to these loadings. In the present work, it is implemented digital image correlation using one laser-beam and the speckles created by its reflection to describe the mechanical behavior of fiber-reinforced composites submitted under compression test. Composites were tested in two set of arrays: the first was done with fibers orientated parallel to the load and the second was done with fibers randomly orientated, as it is known that the stress-strain evolution change according to the orientation of the fibers. Our method allows us to evaluate the heterogeneous strain evolution observed during the tests. Validity of optical strain-measurements is assessed against the results of an universal testing machine, a good correlation was found by comparing the results.

Keywords: Laser speckle; In-plane strain measurement; Digital image correlation; Compression test; Composite materials

Introduction

It is important to measure local strain and stress distributions for understanding the mechanical properties of structural materials. The stress-strain diagram helps to understand materials under loads [1]. There are two methods to obtain those diagrams: contact and non-contact; in the former case, mechanics excels doing physical tests such as compression test, in which a material is placed in the universal machine, a continuous load is applied to it and the resulting deformation is measured [2]. Optical methods are also used as an invasive way to determine residual stress, in-field displacements and strain, in which hole-drilling is one of the most used techniques, developed in 1930 by Mathar [3]. Nowadays this technique is standardized by ASTM [4]. When a laser light felt on a matt surface such as paper or rough-like material, a speckle pattern is formed and a high-contrast grainy pattern will be reflected. This effect was called â€œgranularityâ€ by Rigden and Gordon [5]. The speckle pattern is formed when coherent light is reflected from a rough surface or when light is propagated through a medium with random refractive index fluctuations [6]. The simplest image matching procedure is cross-correlation (CC) that can be performed either in physical space [7,8]; in Fourier space by using the Fast Fourier Transform (FFT), one can evaluate the CC function very quickly [9]. Anuta took advantage of the high speed of FFT algorithm doing digital multispectral and multi-temporal statistical pattern-recognition [10]. Kuglin and Hines observed that information about the displacement of one image with respect to another is included in the phase component of the cross-power spectrum of the images [11].

Composite materials are widely used in structures as they can reach high loads and strain measurements had been studied through different techniques: one of them is the strain gauges used to analyze the strain [12], the electron MoirÃ© method used to measure the strain distribution [13] and fiber optics sensors for strain measurements [14]. The development of non-destructive testing methods is the main challenge for the assessment of structural elements in existing constructions. This paper presents an alternative method for measuring deformation in composite materials, in which we use a laser beam focusing on the cross-section of our sample which is under a compression test; the studied material is formed by ARMEX plus concrete. As the reflection of the laser is a speckle pattern, we need to study it by the means of Digital Image Correlation (DIC) and the Infinitesimal Strain Tensor in order to get in-field displacements measurements. We calculate the accuracy, error and sensitivity of the method, as well as a theoretical demonstration of our phenomenological process; assessing that the present work would be a cheap technique as it only uses one laser beam for stress-strain measurements.

In section 4 we put forward concepts that are used in the present work. Section 4.1 explains the correlation technique and the equations we are following, in section 4.2 we put forward the equations involving the composite materials study, including the well-known mixture law, section 4.3 shows the stress-strain relation with the Youngâ€™s modulus and how the stress is calculated in a composite material and in section 4.4 we explain a theoretical analysis of the physical phenomena. Experimental set-up is presented in section 5, which includes the dimensions of our samples, how compression tests are done and how DIC is taking place. Finally the results and discussion are shown in section 6, in which there are two plots of interest: the stress-strain diagram which is obtained from the universal machine and the DIC plot which is programmed using a code written in Matlab.

Developments

Correlation technique

Digital image correlation is an optical method that examines image data taken while samples are during mechanical tests. This technique consists on capture consecutive images with a digital camera in order to evaluate the change in surface characteristics and understand the behavior of the specimen while it is subjected to a continous axial load.

***Corresponding author:** Aguilar PAM, Department of Engineering, Autonomous Univiersity of Morelos State, Mexico, Tel: 527773297000; E-mail: pmarquez@uaem.mx

Received September 20, 2016; **Accepted** September 28, 2016; **Published** October 10, 2016

Citation: Heredia AS, Aguilar PAM, Ocampo AM (2016) Stress-Strain Characterization in Fiber-Reinforced Composites by Digital Image Correlation. J Material Sci Eng 5: 286. doi:10.4172/2169-0022.1000286

It is well known that for correlation is needed to obtain the spectrum between two images; let's call U and V a pair of 2-D images, where U represents the reference image and V the displaced image [15], therefore is taken the FFT form both and cross-spectrum is defined by:

$$C_S(u,v) = F(u,v) \cdot G^*(u,v) \quad (1)$$

where F is the Fourier transform of the first image and G^* is the complex conjugate Fourier transform of the second; once obtained the spectrum, it is taken the cross-correlation between those images, defined by:

$$C_C = F^{-1}[F(U) \cdot G^*(V)] \quad (2)$$

The use of FFT requires that images U and V are the same size and have dimensions that are powers of 2. In the present work, we analyze 2^{10} square images in order to map a bigger area of the whole image and the shift $\delta x = (\delta y)$ between two consecutive images is 128 pixels in order to get a better result. These two parameters define the mesh formed by the images used to describe the displacement field [16].

Stress-strain analysis in composite materials

When unidirectional continuous-fiber laminate is loaded in a direction parallel to its fibers, the longitudinal modulus E_{11}can be estimated from its constituent properties by using the well-known rule of mixtures:

$$E_{11} = E_f V_f + E_m V_m \quad (3)$$

where E_f is the fiber modulus, V_f is the fiber volume percentage, E_m is the matrix modulus and V_m is the matrix volume percentage [17]. We treat the composite material as acting in a purely elastic manner and neglect the viscoelastic effects of the matrix; Hookeâ€™s Law then can be applied:

$$\sigma_f = E_f \varepsilon_f \quad (4)$$

$$\sigma_m = E_m \varepsilon_m \quad (5)$$

Therefore, the longitudinal tensile strength σ_{11} also can be estimated by:

$$\sigma_{11} = \sigma_f V_f + \sigma_m V_m \quad (6)$$

Where σ_f and σ_m are the ultimate fiber and matrix strengths respectively. As properties of fibers dominate for all practical volume percentage, the values of the matrix can be ignored and Eq. (6) is reduced:

$$\sigma_{11} \approx \sigma_f V_f \quad (7)$$

This type of composite materials is called fiber-reinforced composites (FRC), which can be classified as either continuous or discontinuous; generally, the highest strength is obtained with continuous reinforcement. When FRC are used with continuous and aligned fibers orientated parallel to the load, the efficiency of the reinforcement is 98 % as Eq. (7) shows, but when fibers are randomly orientated through the 3-D space, the efficiency decreases to 1/5 of its value [18].

Compression tests

Physical tests are used in order to know mechanical properties of materials and compression test is one of these tests which enable the user to understand the behavior of a material under a continuous axial load; from this test we obtain the stress-strain diagram [2]. In this work we made a mixture of sand-cement with a ratio of 3x1 respectively with dimensions of 5×5×4.5 cm. and they undergo into compression test according to ASTM E-9 [19]. We did two set of tests, one for fibers parallel orientated and the other for randomly orientated; both of them were performed with a speed ratio of 0.5 mm/s, the first up to 140 GPa and the second up to 7 GPa approx. Since we are working on the elastic part of the diagram, therefore we can apply Hooke's law:

$$\sigma = E \cdot \varepsilon \quad (8)$$

where σ is the stress, E is the Youngâ€™s modulus of the material: 53 GPa when fibers are aligned parallel to the load and 2.2 GPa when they are randomly aligned, both experimentally obtained by the universal machine and ε is the dimensionless strain.

In DIC procedure, when the same reference picture is used, it is not possible to measure large displacements in a sequence of pictures, but when they remain small enough it is possible to assume the first image as the reference for the whole analysis. In the present work, we work with deformations less than two millimeters. It is well-known that the infinitesimal strain tensor ε_c is well adapted to small displacements and it can be evaluated as:

$$\varepsilon_c = \frac{1}{2}(R + R^T) - 1 \quad (9)$$

where ε_c is the strain, R is an orthogonal second rank tensor and R^T implies transpose. Taking this outset, we show the theoretical results of strains: ε obtained by the universal machine and ε_c obtained by DIC technique.

Theoretical analysis

In the present work, we are working with a laser beam with an output tye of TEM_{00} which corresponds to a Gaussian beam, this kind of beam has an intensity distribution of:

$$I(r) = I_0 exp[\frac{-2r^2}{w^2}] \quad (10)$$

where $r = (x^2 + y^2)^{1/2}$ and w is the spot size and depends on the z-coordinate [20]. The equation of such beam is deduced from Helmholtz equation and is represented by [21]:

$$E(r,z) = A\frac{w_0}{w(z)} exp[\frac{-r^2}{[w(z)]^2} + \frac{kr^2}{2R(z)} + kz - \eta(z)] \quad (11)$$

where w_0 is the beam waist, $w(z)$ is the beam spot size, $R(z)$ is the curvature radius of the spherical waves and $\eta(z)$ is the beam phase angle [22]. And the intensity distribution of a Gaussian beam according to Eq. (11) is:

$$I(r,z) = I_0 \frac{w_0^2}{[w(z)]^2} exp[\frac{-2r^2}{[w(z)]^2}] \quad (12)$$

Gaussian beams are able to pass through different media; the light reflection occurs when it arrives to the boundary separating two media of different optical densities and some of the energy is reflected back into the first medium [23], taking this outset, our laser-beam strikes a rough material and the reflection can be studied as a speckle pattern. The ratio between the intensity of the reflected beam and the incident beam is called reflectivity R and is expressed by:

$$R = \frac{I_r}{I_i} \quad (13)$$

where I_r and I_i are the reflected and incident beams respectively; when a beam pass through the media, there exist transmissivity T and according to the conservation law of energy [24]:

$$T + R = 1 \quad (14)$$

In the present work, as we are working with solid materials, the transmissivity is zero, thus we can assume that:

$$I_i \cdot R = I_r \quad (15)$$

for R ≤ 1, invoking Fresnel diffraction equation and according to cross-spectrum analysis Eq. (1), taking U as a speckle pattern with an intensity distribution [25], expanding formally and changing coordinates we obtain

$$F(u,v)=\iint_{-\infty}\frac{1}{4\pi\sigma^2}exp[\frac{-(x^2+y^2)}{2\sigma^2}]exp^{-i2\pi(ux+vy)}dxdy \quad (16)$$

$$U(\rho:t)=\frac{1}{4\sigma^2}exp[\frac{\pi^2\sigma^2}{2}\rho^2] \quad (17)$$

Being $U(\rho:t)$ the first image Fourier transform at an initial time t_0 ; the same process is done for $V(\rho:\Delta t)$, where V is the second image Fourier transform at a time t_1 and cross correlation is defined by:

$$CC=[\frac{1}{4\sigma^2}]^2exp^{i2\pi(\Delta x+\Delta y)} \quad (18)$$

Finally it is taken the correlation phase from the exponential and infinitesimal strain tensor takes place obtaining in-field measurements. From Eq. (18) is possible to see that the relation keep a Gaussian form, thus this case can be studied as a linear behaviour.

Experimental Set-Up and Data Processing

Six probes were made by adding 3×1 sand-cement mixture and each with four fibers of ARMEX, the fibers of three of them were randomly orientated in order to compare and study if the technique would be accurate in the measurement of a possible human error. The samples were placed in the universal testing machine in order to begin the compression tests. A diagram of this method is shown schematically in Figure 1a. The output of a Diode-Pumped Solid-State laser (L) with a wavelength λ=532 nm and power of 220 mW [26], is propagated through a positive lens (l) is placed in front of the sample (Sa) in order to irradiate the cross-section face and the scattering reflection impacts a screen (Sc) which is placed aside the laser beam; the material is first completely flat and it is compressed by the machine (M). During the compression tests, the speed of the compression load was 0.5 mm/s with duration of 20 minutes approximately and while they were taking place the speckle reflection was recorded with a high resolution video camera (Vc).

Once the video is recorded, Video to JPG free software is used to divide it into frames in order to load each image and process it, this software enable us to turn our videos with an average of 54 frames per second. Therefore a program is written in Matlab for Digital Image Correlation (DIC). The cross-correlation calculation is described below: in Figure 2a it is shown how the code loads the image and it is converted into a gray-scale image as it is shown in (b); the image is crop into a 1024 × 1024 in order to begin the FFT analysis of all the images, taken the first as the reference; from the second image and forward, they are considered as deformed images.

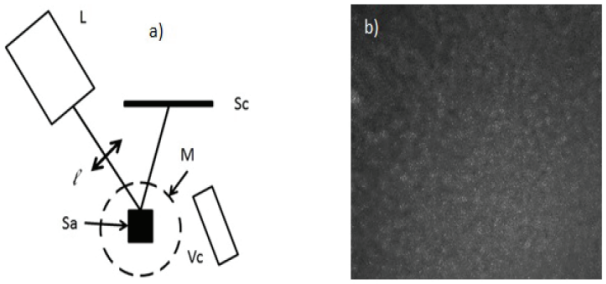

Figure 1: Experimental set-up (a) material with no strain; (b) speckle photogram.

Once it is done the cross correlation technique we obtain the phase component as Kuglin and Hine. Therefore we apply a shift between each interval $\delta x=\delta y$ 128 pixels as is shown in Figure 3.

The first strain measured by the universal machine is 0.002 while cross correlation technique allows us to measure 0.002162; the shear component is equal to or less than 1.6×10^{-4}. It has been reported that for pure rotation measurements they obtained 2×10^{-4} [16].

Results and Discussion

In the section above, we mentioned that six samples were prepared for compression test, the first three probes that are shown below are done with continuous and aligned fibers orientated parallel to the load, for each one has been obtained two graphs of interest, the strain diagram is shown in Figure 4 and the DIC plot which is shown in Figure 5, which correspond to the first sample.

In Figure 4 we plot the strain diagram obtained from the machine and in Figure 5 we plot the stress-strain diagram from the experimental results obtained by Eq.(9). For both graphs we see a linear behavior. In the next Figure 6 we compare the real strain and the experimental data obtained, also some statistical results are shown in Table 1.

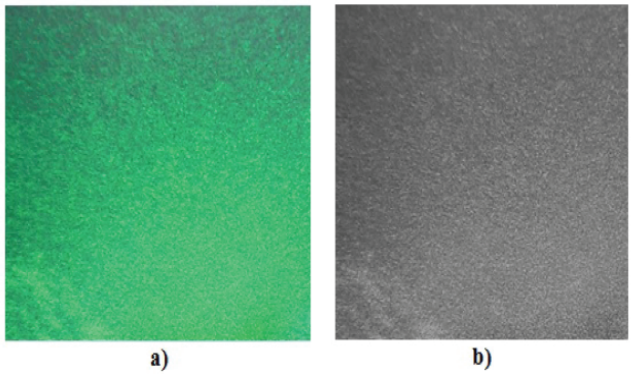

Figure 2: Cross correlation technique: (a) loaded image; (b) grey-scale image.

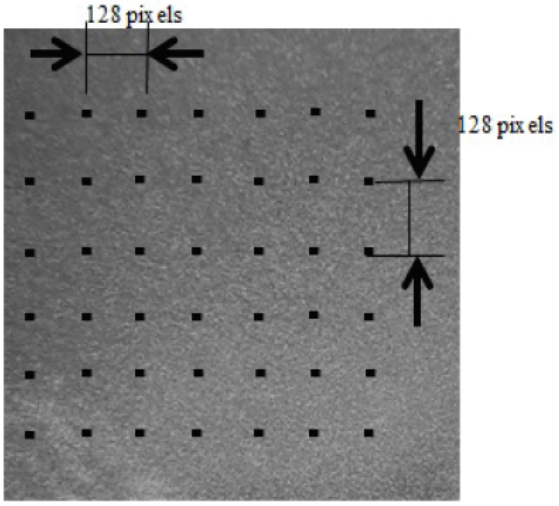

Figure 3: Displacement contours δx = δy = 128 pixels.

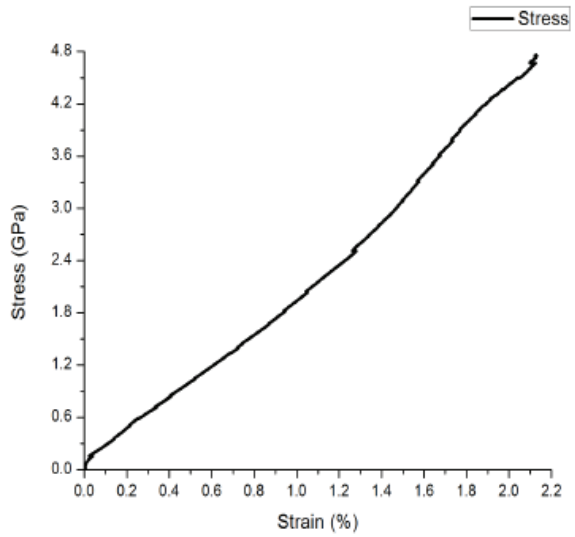

Figure 4: Real stress-strain diagram.

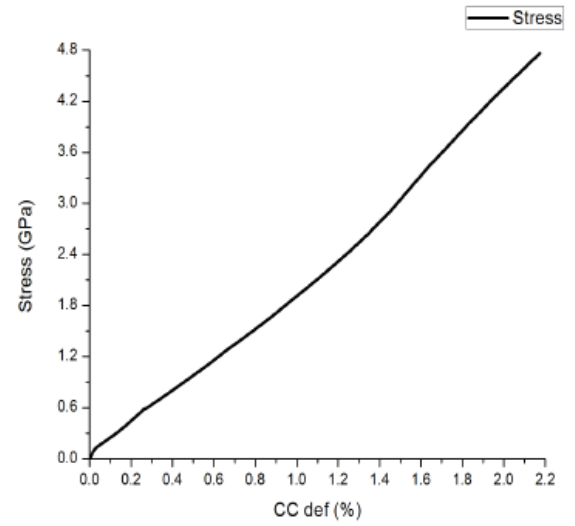

Figure 5: Experimental stress-strain diagram.

In Figure 6 we plot both graphs of interest, stress-strain from the machine and cross-correlation strains from Eq.(8) (black) and from Eq.(9) (red) respectively. These results are shown for each sample; in Table 1 is shown the statistics of this test, it was observed that there is a good correlation obtaining 5.4% error from the real strain measurement.

In Figure 7 is represented the second test and is shown both plots of interest; Table 2 summarizes it showing the statistics of this test, it was observed a better correlation than sample 1 obtaining 4% error from the real strain measurement.

The test for the third sample is shown in Figure 8, in which is shown both plots of interest and Table 3 summarizes showing the statistics of this test, it was observed a simmilar behaviour than sample 2 obtaining 4.6% error from the real strain measurement.

Table 4 summarizes these tests performed with fibers aligned and

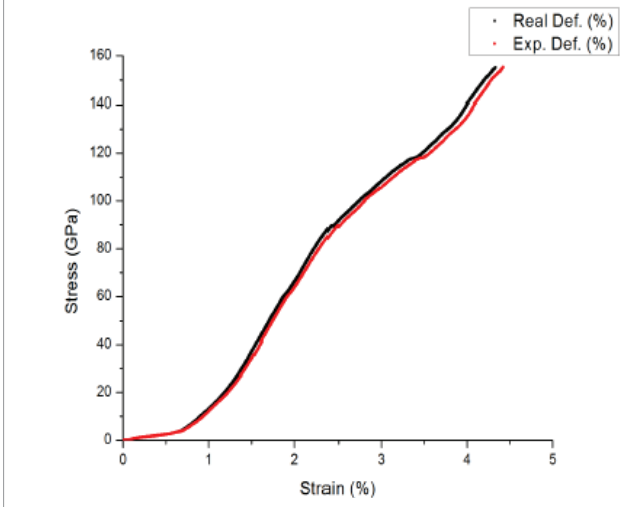

Figure 6: Comparison between stress-strain diagrams for sample 1.

Young's Modulus E	50 +/- 1.8 GPa
% difference from 52 GPa	5.4%
Standard deviation	2.45

Table 1: Statistical results for sample 1 during the compression test and cross-correlation analysis; fibers aligned and parallel orientated to the load.

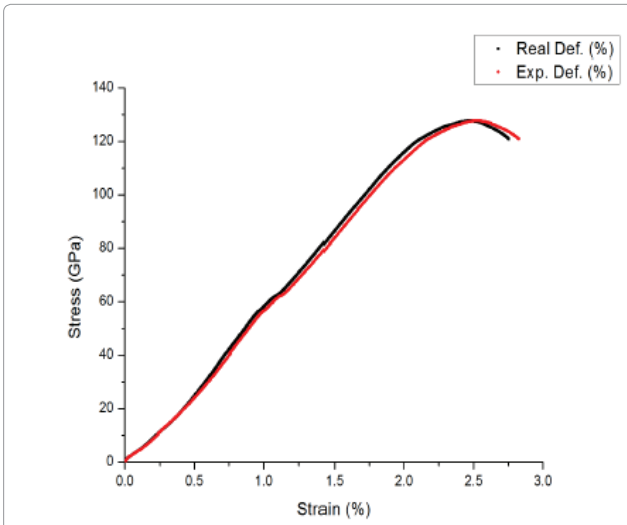

Figure 7: Comparison between stress-strain diagrams for sample 2.

Young's Modulus E	51 +/- 1 GPa
% difference from 52 GPa	4%
Standard deviation	1.5

Table 2: Statistical results for sample 2 during the compression test and cross-correlation analysis; fibers aligned and parallel orientated to the load.

parallel orientated to the load, we can assume that the mean accuracy is 95.3%. Now we present the results for the three composites with fibers randomly orientated to the load. In Figure 9 we plot both plots of interest, stress-strain from the machine and cross-correlation strain measurements. These results are shown for each sample in Table 5 shows the statistics of the first test, it is appreciate a better correlation than parallel ones, obtaining 3% error from the real strain measurement. By

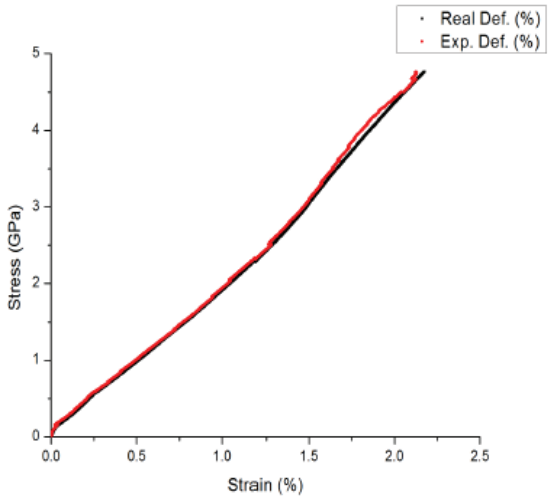

Figure 8: Comparison between stress-strain diagrams for sample 3.

Young's Modulus E	50.5 +/- 1.5 GPa
%difference from 52 GPa	4.6%
Standard deviation	1.95

Table 3: Statistical results for sample 3 during the compression test and cross-correlation analysis; fibers aligned and parallel orientated to the load.

Sample	Accuracy	Mean error
	94.6%	5.4%
	96%	4%
	95.4%	4.6%

Table 4: Accuracy and error of the three tests; fibers aligned parallel to the load.

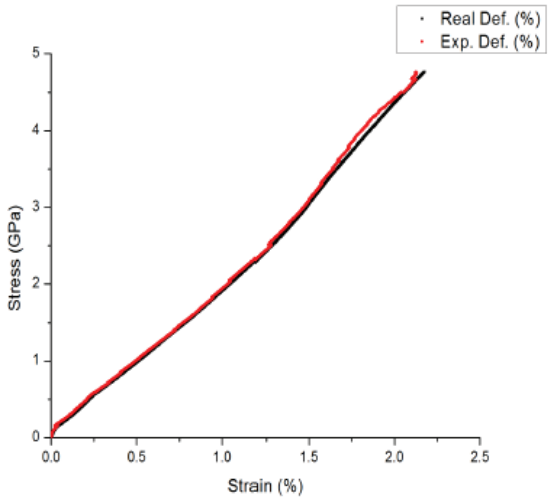

Figure 9: Comparison between stress-strain diagrams for sample 1.

Young's Modulus E	1.9 +/- 0.04 GPa
%difference from 2 GPa	3%
Standard deviation	1.2

Table 5: Statistical results for sample 1 during the compression test and cross-correlation analysis; fibers randomly orientated to the load.

doing a second test with fibers randomly orientated, it was observed not as good correlation than sample 1 obtaining 5% error from the real strain measurement. In Figure 10 we can see both plots of interest and Table 6 summarizes showing the statistics of this test.

A third test was done and Figure 11 shows both plots of interest, Table 7 summarizes showing the statistics of this test, it was observed a similar correlation to sample 1 obtaining 3% error from the real strain measurement. Table 8 summarizes these tests performed with fibers randomly orientated to the load, we can assume that the mean

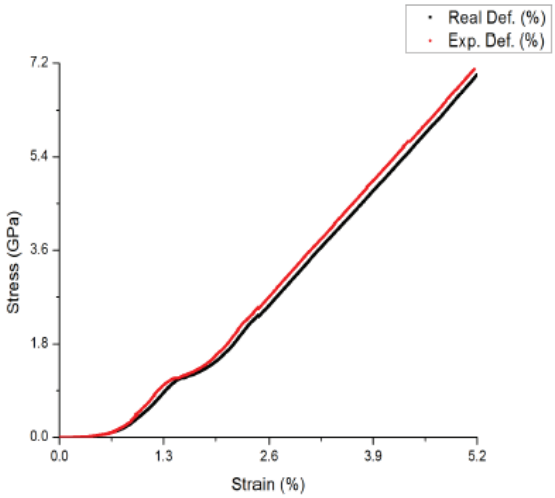

Figure 10: Comparison between stress-strain diagrams for sample 2.

Young's Modulus E	1.7 +/- 0.4 GPa
%difference from 2 GPa	5%
Standard deviation	1.9

Table 6: Statistical results for sample 2 during the compression test and cross-correlation analysis; fibers randomly orientated to the load.

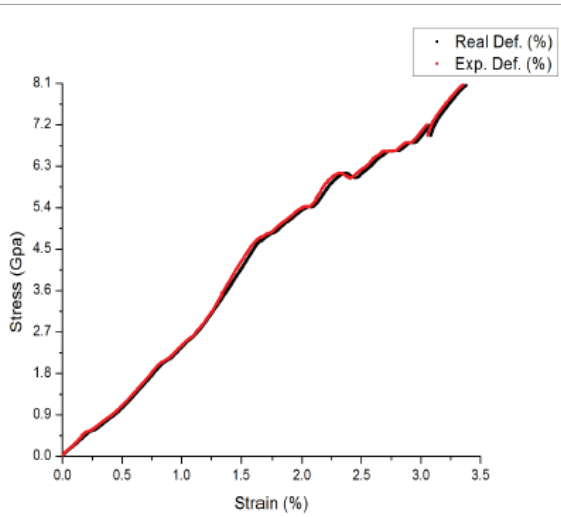

Figure 11: Comparison between stress-strain diagrams for sample 3.

Young's Modulus E	1.89 +/- 0.05 GPa
%difference from 2 GPa	3%
Standard deviation	1.92

Table 7: Statistical results for sample 3 during the compression test and cross-correlation analysis; fibers randomly orientated to the load.

Sample	Accuracy	Mean error
	97%	3%
	95%	5%
	97%	3%

Table 8: Accuracy and error of the three tests; fibers randomly orientated to the load.

accuracy is 96%. By comparing the average strain determined for 6 different specimens with the compression stress values measured with the load cell, it was demonstrated that the present technique can measure the relative strain with an average uncertainty of 5% for strain measurements of composite materials with fibers parallel orientated to the load and 4% for strain measurements of composite materials with fibers randomly orientated to the load.

Conclusions

It was measured the strain of two composite materials under a compression test using one laser-beam, its speckles reflection and digital image correlation treatment, we obtain 95% of accuracy for strain measurements in composites with fibres parallel orientated to the load and 96% of accuracy for strain measurements in composites with fibres randomly orientated to the load. Also we obtained 1.05×10^{-4} sensitivity, which is less than the reported 2×10^{-4}. We demonstrate that cross-correlation plus speckle metrology could be a reliable technique for measuring strain in composite materials under standardized compression tests.

Acknowledgements

Alonso Salda Ã ± a Heredia wants to thank CONACYT for the grant No. 360140.

References

1. Beasley F, Beasley DE (2011) Theory and design for mechanical measurements (5th edn.) John Wiley & Sons, USA.
2. Gere J, Goodno B (2009) Materials mechanics (7th edn.) Cengage Learning, Mexico.
3. Mathar J (1934) Determination of initial stresses by measuring the deformation around drilled holes. Transactions ASME 56: 249-254.
4. ASTM (2008) Determining residual stresses by the hole-drilling strain gage method. ASTM Standard Test Method E837-08. American Society for Testing and Materials, West Conshohocken, PA.
5. Rigden JD, Gordon EI (1962) The granularity of scattered optical laser light. Proceedings of the Institute of Radio Engineers 50: 2367-2368.
6. Dainty JC, Ennos AE, Francon M, Goodman JW, McKechnie TS, et al. (1975) Laser speckle and related phenomena. Springer-Verlag Berlin Heidelberg.
7. Peters WH, Ranson WF (1982) Digital image techniques in experimental stress analysis. Opt Eng 21: 427-431.
8. Sutton MA, Mc Neill SR, Helm JP, Chao YJ (2000) Advances in two dimensional and three dimensional computer vision. Photomechanics 77: 323-372.
9. Chen DJ, Chiang FP, Tan YS, Don HS (1993) Digital speckle-displacement measurement using a complex spectrum method. Appl Opt 32: 1839-1849.
10. Anuta PE (1970) Spatial registration of multispectral and multitemporal digital imagery using fast Fourier transform techniques. IEEE Trans Geosci Electron 8: 353-368.
11. Kuglin CD, Hines DC (1975) The phase correlation image alignment method. Proc Int Conf Cybernetics and Society, Japan.
12. Stanciu A, Cotoros D, Baritz M, Rogozea L (2010) Analysis by strain gauges of the strains in a composite material. Recent advances in signal processing, robotics and automation. pp: 254-257.
13. Satoshi K, Yoshihisa T, Kimiyoshi N, Yutaka K (2011) Measurement of strain distribution of composite materials by electron moire method.
14. Domanski AW, Bieda M, Lesiak P, Makowski P, Szelag M, et al. (2013) Polarimetric optical fiber sensors for dynamic strain measurement in composite materials. Acta Phys Pol A 124: 399- 401.
15. Pradille C, Bellet M, Chastel Y (2010) A laser speckle method for measuring displacement field. Application to resistance heating tensile test on steel. Applied Mechanics and Materials 24: 135-140.
16. Chevalier L, Calloch S, Hild F, Marco Y (2001) Digital image correlation used to analyze the multiaxial behavior of rubber-like materials. Eur J mech A/solids 20: 169-187.
17. Campbell FC (2010) Structural composite materials. ASM International.
18. Mitchell BS (2004) An introduction to materials engineering and science. John Wiley & Sons, USA.
19. ASTM E-9, ICS Number Code 77.040.10, Mechanical testing of metals.
20. Sirohi RS (2009) Optical methods of measurement wholefield techniques (2nd edn.) Taylor and Francis Group, USA.
21. Alda J (2003) Laser and gaussian beam propagation and transformation. Encyclopaedia of optical Engineering. pp: 999-1013.
22. Yariv A (1990) Quantum Electronics (3rd edn.) John Wiley & Sons, USA.
23. Wood R (1988) Physical Optics (3rd edn.) Optical Science of America, Washington DC.
24. Born M, Wolf E (1970) Principle of optics (4th edn.) Pergamon Press, U.K.
25. Goodman JW (1976) Some fundamental properties of speckle. J Opt Soc Am 66: 1145-1150.
26. (2015) Laser Product Datasheet generated on.